© 2019. Published by The Company of Biologists Ltd | Journal of Cell Science (2019) 132, jcs225789. doi:10.1242/jcs.225789

RESEARCH ARTICLE

PCNT is critical for the association and conversion of centrioles to centrosomes during mitosis

Jaeyoun Kim, Jeongjin Kim and Kunsoo Rhee*

ABSTRACT

A centrosome consists of a pair of centrioles and pericentriolar material (PCM). We manipulated expression of PCNT, a key PCM protein, and investigated roles of PCM in centriole behavior during mitosis. Deletion of *PCNT* had little effect on interphase centrosomes. However, centrioles in *PCNT*-deleted mitotic cells prematurely separated and frequently amplified, revealing that centrioles are limited within the spindle poles by PCNT during mitosis. It is known that specific cleavage of PCNT is necessary for centriole separation during mitotic exit. We observed delayed centriole separation in the G0 phase when a non-cleavable mutant form of PCNT was removed or when PCNT was artificially cleaved by TEV protease. Furthermore, a daughter centriole converts to a mother centriole only after experiencing both mitotic exit and specific PCNT cleavage. Based on these results, we propose that a centriole pair disengages upon entering mitosis but remains associated with the surrounding PCM proteins throughout mitosis. During mitotic exit, specific cleavage of PCNT induces PCM disintegration. As a result, a daughter centriole separates from the mother centriole and converts to a young mother centriole.

KEY WORDS: Centrosome, Centriole separation, Centriole disengagement, Centriole-to-centrosome conversion, Pericentriolar material, Pericentrin, Mitosis

INTRODUCTION

In mammalian centrosomes, a pair of centrioles is surrounded by a multilayered protein matrix called pericentriolar material (PCM). Centrioles duplicate and segregate in close association with the cell cycle. A daughter centriole assembles at a perpendicular angle to the mother centriole during G1/S phase. When cells enter mitosis, centrosomes become enlarged with the accumulation of PCM and emanate a great number of microtubules to function as spindle poles. At the end of mitosis, PCM disintegrates, and centrioles separate from each other. At this time, a daughter centriole becomes a young mother centriole, acquiring the abilities to recruit PCM and to assemble a new daughter centriole in the next cell cycle round (Wang et al., 2011).

Mechanistic details of the centrosome cycle have been intensely investigated (Loncarek and Bettencourt-Dias, 2017; Nigg and Holland, 2018). PLK4 is a master regulator of the initiation of centriole assembly in *Caenorhabditis elegans*, *Drosophila melanogaster* and human (O'Connell et al., 2001; Bettencourt-Dias et al., 2005; Habedanck et al., 2005). PLK4 activity fluctuates in a cell cycle-dependent manner, so that it is low at G1 phase, increases at G1/S transition and remains high until mitotic exit (Holland et al., 2010). When overexpressed, PLK4 can induce multiple centriole precursors surrounding a single parental centriole (Habedanck et al., 2005). It is known that CEP192 and CEP152 sequentially serve as scaffolds for the recruitment of PLK4 to the mother centriole (Kim et al., 2013). Once PLK4 is recruited, it phosphorylates STIL and other centrosomal proteins to initiate centriole assembly (Kitagawa et al., 2009; Dzhindzhev et al., 2014; Ohta et al., 2014; Arquint et al., 2015; Kratz et al., 2015; Moyer et al., 2015; Arquint and Nigg, 2016; Lee et al., 2017). SAS6 is a key structural component of a cartwheel that establishes ninefold symmetry of the triplet microtubule blades in a nascent centriole (Kitagawa et al., 2011; van Breugel et al., 2011).

After a daughter centriole is liberated from the mother centriole during mitotic exit, it follows a series of changes, named centriole-to-centrosome conversion, to become a young mother centriole (Wang et al., 2011). A young mother centriole can initiate PCM recruitment and can be a template for a new centriole (Wang et al., 2011). A prerequisite step for the centriole-to-centrosome conversion may be the recruitment of CEP152, which functions as a scaffold for PLK4 in the next round (Cizmecioglu et al., 2010; Dzhindzhev et al., 2010; Hatch et al., 2010). Sequential recruitment of centriolar proteins, such as CEP135, CEP295 and CEP192, precede the recruitment of CEP152 (Izquierdo et al., 2014; Fu et al., 2015; Chang et al., 2016; Tsuchiya et al., 2016). That is, preparation for centriole duplication is already initiated during mitosis.

Pericentrin (PCNT) is one of the major scaffold proteins in PCM (Doxsey et al., 1994). Mutations in *PCNT* cause serious congenital abnormalities, such as microcephalic osteodysplastic primordial dwarfisms, ciliopathies and mental disorders (Delaval and Doxsey, 2008; Rauch et al., 2008). In an interphase centrosome, PCNT is radially arranged with the C-terminal end near the centriole (Lawo et al., 2012; Mennella et al., 2012; Sonnen et al., 2012). It is proposed that other PCM proteins are associated with PCNT to form the multilayered toroid structure of PCM in interphase cells (Lawo et al., 2012; Mennella et al., 2012). PCM in mitotic cells is less organized, but a significant amount of PCNT is recruited to the mitotic centrosome (Woodruff et al., 2014; Conduit et al., 2015). PCNT is also required for recruitment of other PCM proteins to make mitotic centrosomes function as spindle poles (Doxsey et al., 1994; Kim and Rhee, 2014). PLK1 phosphorylation of PCNT is important for mitotic PCM recruitment (Lee and Rhee, 2011). At the end of mitosis, PCNT is specifically cleaved by separase, which is an essential step for centriole separation (Lee and Rhee, 2012; Matsuo et al., 2012; Kim et al., 2015). However, it remains to be investigated how centriole separation is induced by PCNT cleavage.

In this work, we elaborately manipulated a range of PCNT functions to determine their roles in mitotic centrosomes. We revealed that PCNT is essential for centriole association and for limiting centriole amplification in mitotic cells, while it has minimal

Department of Biological Sciences, Seoul National University, Seoul 08826, Korea.

*Author for correspondence (rheek@snu.ac.kr)

Jaeyoun Kim, 0000-0001-8809-8054; Jeongjin Kim, 0000-0002-6959-8544; K.R., 0000-0002-5051-876X

Received 22 September 2018; Accepted 14 February 2019

Journal of Cell Science (2019) 132, jcs225789. doi:10.1242/jcs.225789

effects on interphase centrosomes. Specific cleavage of PCNT is a necessary step for centriole-to-centrosome conversion as well as for centriole separation during mitotic exit.

RESULTS

Generation of *PCNT*-deleted cells

We and others have previously reported that specific cleavage of PCNT is a necessary step for centriole separation during mitotic exit (Lee and Rhee, 2012; Matsuo et al., 2012). This led us to propose that the mother and daughter centrioles might be held together within PCM during mitosis. To test this hypothesis, in earlier work we depleted PCNT with siRNA transfection and analyzed the phenotypes. We observed that PCNT-depleted cells had defects in bipolar spindle formation with reduced levels of PCM proteins in their spindle poles. However, we had not previously observed any significant increase of premature centriole separation in PCNT-depleted mitotic cells (Lee and Rhee, 2011). We recently repeated the experiments knocking down PCNT in both HeLa and U2OS cells. The results showed that premature centriole separation slightly increased in both cell lines (Fig. S1). We also noticed that a faint signal of PCNT was still detected even after siRNA transfection (Fig. S1a,e). Therefore, we decided to generate *PCNT* knockout cell lines and determine premature centriole separation in the *PCNT*-deleted cell lines.

The *PCNT*-deleted HeLa cell lines were generated with the CRISPR/Cas9 method (Fig. S2). Deletion of the *PCNT* gene was carried out in the *TP53*-deletion background since the p53 pathway is frequently activated after deletion of centrosomal genes (Fong et al., 2016; Lambrus et al., 2016; Meitinger et al., 2016). In fact, we observed that most of the *PCNT*-deleted cell lines did not grow unless *TP53* was simultaneously deleted (data not shown). Immunoblot analysis revealed that both the PCNT- and p53-specific bands were undetectable, confirming that both *PCNT* and *TP53* genes were deleted (Fig. 1A).

Deletion of *PCNT* caused failure in recruitment of PCM into mitotic centrosomes

We performed immunocytochemistry to determine the centrosomal levels of selected PCM proteins in *PCNT*-deleted cells. As expected, the centrosomal signal of PCNT was undetectable in the *PCNT*-deleted cells (Fig. 1B,C). However, the centrosomal levels of other PCM proteins, such as CEP215, CEP192 and γ-tubulin, were unaffected or slightly diminished in the *PCNT*-deleted interphase cells (Fig. 1B,D–F). These results suggest that PCNT is dispensable for PCM formation in interphase centrosomes.

Next, we determined the effects of *PCNT* deletion on mitotic centrosomes. The cells were treated with thymidine followed by S-trityl-L-cysteine (STLC) to arrest the cell cycle at prometaphase (Fig. 1G) (Seo et al., 2015). Under these conditions, most cells started to enter mitosis 9 h after thymidine release, so they should be arrested at prometaphase for the final few hours. Again, centrosomal PCNT was absent (Fig. 1H,I). However, unlike in interphase centrosomes, centrosomal levels of CEP215, CEP192 and γ-tubulin were significantly reduced in prometaphase-arrested cells (Fig. 1H,J–L). Additionally, we determined centrosomal signals of CEP215 and CEP192 in *PCNT*-deleted cells at interphase and mitosis. We observed that the centrosomal levels of CEP215 and CEP192 increased when cells entered mitosis (Fig. 1M–O). However, such increment was absent in *PCNT*-deleted mitotic cells (Fig. 1M–O). These results reinforce previous reports that PCNT plays a critical role in PCM accumulation into the centrosome during mitotic entry (Doxsey et al., 1994; Lee and Rhee, 2011; Kim and Rhee, 2014).

PCNT deletion resulted in defects in bipolar spindle formation

Even when *PCNT*-deleted cell lines could be maintained for a sufficient time period to perform experiments, a fraction of the cells were observed to undergo apoptosis (Fig. S3). Therefore, we suspected that deletion of *PCNT* is harmful to cell survival. We determined spindle formation defects in cells enriched at M phase with thymidine–RO3306 block and release (Fig. 2A). The results showed a slight but significant increase in mono- or multipolar spindles in the *PCNT*-deleted cells (Fig. 2B,C). For rescue experiments, we generated ectopic $PCNT^{WT}$ in which a destabilization domain (DD) is included for controlled degradation with a small molecule, shield1 (DD–FLAG–PCNT–Myc) (Banaszynski et al., 2006; Egeler et al., 2011). Expression of the ectopic PCNT was under control of the promoter of which the activity is induced by doxycycline. Ectopic expression of the PCNT protein construct $PCNT^{WT}$ (DD–FLAG–PCNT–Myc) efficiently rescued defects in spindle formation (Fig. 2D; Fig. S4). Unequal distribution of centrioles was detected in *PCNT*-deleted cells even after mitosis (Fig. 2E–G). We also noticed that *PCNT*-deleted interphase cells frequently included abnormal nuclei, such as folded, minute and multiple nuclei (Fig. 2H,I). Such defects were rescued with the introduction of ectopic $PCNT^{WT}$ (Fig. 2J). Furthermore, the cells with abnormal nuclei frequently included improper numbers of centrioles (Fig. 2K,L). These results suggest that PCNT is required for proper spindle formation during mitosis. Following mitosis, most of these spindle pole defects may be corrected, leaving a small number of cells with abnormal nuclei.

Centrioles prematurely separated and amplified in *PCNT*-deleted cells in early mitosis

We collected mitotic cells from actively dividing populations using a mitotic shake-off method and performed immunocytochemistry with antibodies specific to CEP135 and centrin-2 to determine centriole separation (Tsou and Stearns, 2006; Lee and Rhee, 2012). The results showed that centrioles prematurely separated in over 60% of the *PCNT*-deleted mitotic cells (Fig. 3A,B). Furthermore, a significant increase in the number of centrioles was also observed (Fig. 3A,C). Centriole separation and amplification were observed when *PCNT*-deleted cells were accumulated at prometaphase using thymidine–STLC treatment (Fig. 3D–F; Fig. S5). However, the centrioles did not prematurely separate in *PCNT*-deleted interphase cells (Fig. S6). The phenotypes of premature separation and amplification of centrioles were suppressed when the knockout cells were rescued with ectopic $PCNT^{WT}$ (Fig. 3G–I). These results suggest that PCNT is essential for centriole association and for limiting centriole reduplication until the end of mitosis.

It is known that centrioles prematurely separate when cells are arrested at M phase for a prolonged period (Seo et al., 2015; Karki et al., 2017). To determine whether the premature separation of centrioles results from the deletion of *PCNT* or from a prolonged mitotic arrest, we performed time-course experiments (Fig. 3J). The results showed that centriole separation in *PCNT*-deleted cells occurred at 10 h, when the cells were about to reach mitosis (Fig. 3K,L). Centriole amplification was also observed at the same timepoint (Fig. 3K,M). By contrast, centriole pairs in control cells remained associated at 10 h and started to separate at 15 h after thymidine release (Fig. 3K,L). Centriole amplification did not occur in *TP53* knockout control cells (Fig. 3K,M). These results support our conclusion that the absence of PCNT causes premature centriole separation and amplification during mitosis.

To determine whether prematurely separated and amplified centrioles were intact or not, we immunostained the centrioles with

Journal of Cell Science (2019) 132, jcs225789. doi:10.1242/jcs.225789

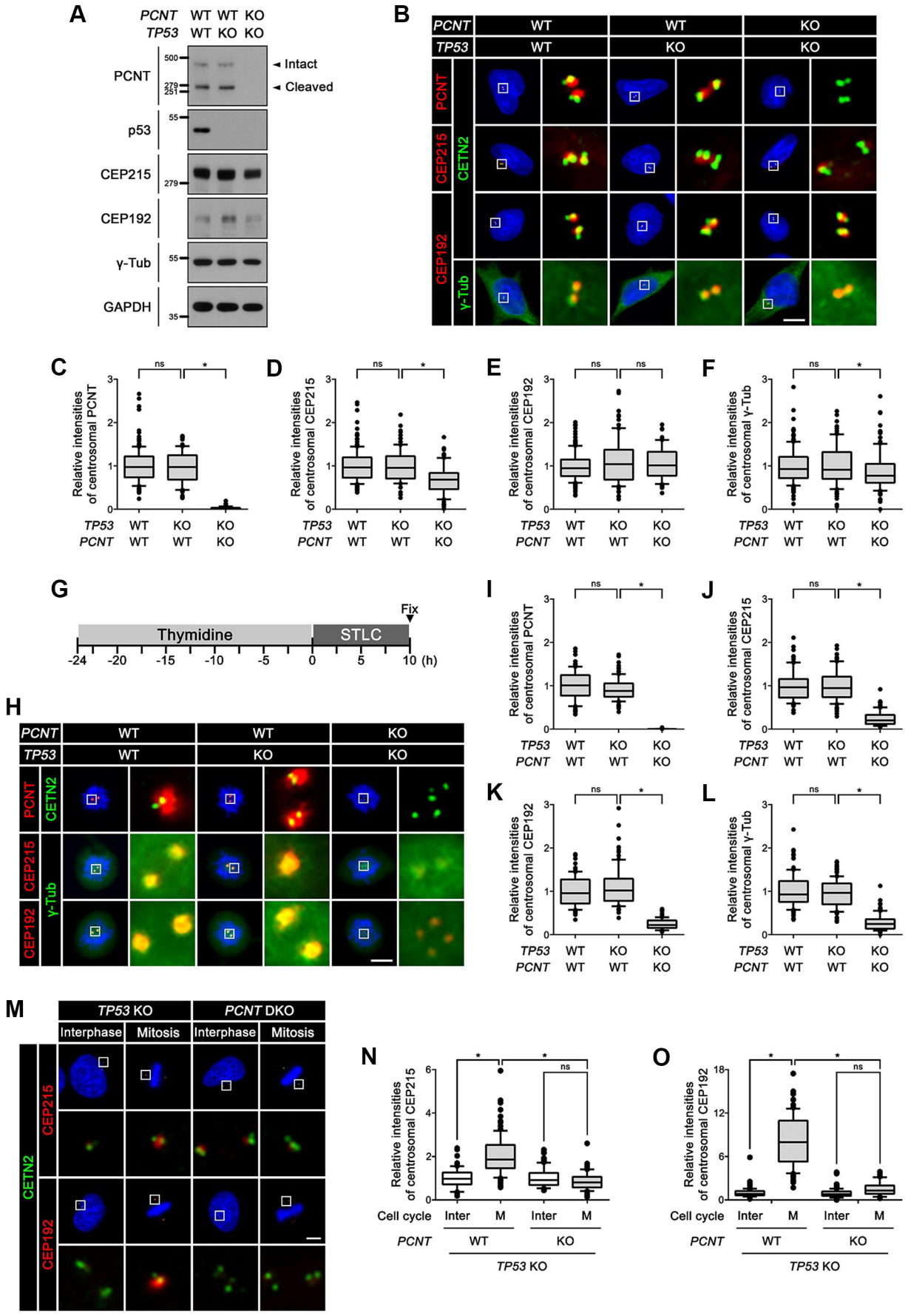

Fig. 1. See next page for legend.

Journal of Cell Science (2019) 132, jcs225789. doi:10.1242/jcs.225789

Fig. 1. Centrosomal levels of selected PCM proteins in *PCNT*-deleted cells. (A) *PCNT* and *TP53* wild-type (WT) or knockout (KO) HeLa cells were subjected to immunoblot analysis with antibodies specific to PCNT, p53, CEP215, CEP192, γ-tubulin (γ-Tub) and GAPDH. (B) Interphase cells were co-immunostained with antibodies specific to centrin-2 (CETN2, green), PCNT (red), CEP215 (red), CEP192 (red) and γ-tubulin (green). Boxed area in left panels is magnified in the right panels. (C–F) Intensities of the centrosomal PCNT (C), CEP215 (D), CEP192 (E) and γ-tubulin (F) signals as shown in B are represented with box and whisker plots (see Materials and Methods for box and whisker definitions). (G) Schematic illustrating how cells were arrested at prometaphase with sequential treatment of thymidine and STLC. (H) Mitotic cells were co-immunostained with the indicated antibodies. (I–L) Intensities of the centrosomal PCNT (I), CEP215 (J), CEP192 (K) and γ-tubulin (L) signals as shown in H are represented with box and whisker plots. (M) Actively dividing wild-type and *PCNT*-deleted cells were co-immunostained with antibodies specific to centrin-2 (CETN2, green), CEP215 (red) and CEP192 (red). Boxed area in upper panels is magnified in lower panels. (N,O) Intensities of the centrosomal CEP215 (N) and CEP192 signals (O) at interphase and mitosis as shown in M are represented with box and whisker plots. (B,H,M) DNA was visualized with DAPI (blue). Scale bars: 10 µm. (C–F,I–L,N,O) >90 centrosomes per group were analyzed in three independent experiments. One-way ANOVA (C–F,I–L) and two-way ANOVA (N,O) were performed for statistical analyses. *P<0.05; ns, not significant.

several centriole markers. First, centriole markers CPAP (also known as CENPJ) and CP110 (also known as CCP110) were detected in all the amplified centrioles (Fig. 4A–C). Second, the majority of the *PCNT*-deleted mitotic cells included a pair of centrioles without centrobin, a marker of daughter centrioles, suggesting that most of the amplified centrioles are daughter centrioles (Fig. 4A,D). Finally, we examined SAS6 signals in naturally dividing cells because SAS6 signals quickly disappear during early mitosis (Strnad et al., 2007). The result showed that ∼20% of mitotic cells included three or more SAS6 signals, suggesting that newly assembled centrioles include a cartwheel structure (Fig. 4E,F). These results strongly suggest that intact daughter centrioles are prematurely generated during mitosis in *PCNT*-deleted cells.

Centrosomal levels of PCNT were critical for centriole separation

There is controversy regarding how mother and daughter centrioles are held together. The cohesin ring complex was initially proposed as a linker that holds mother and daughter centrioles (Schöckel et al., 2011). However, subsequent reports revealed that centrioles remain engaged even in *cohesion*-deleted mutants (Cabral et al., 2013; Oliveira and Nasmyth, 2013; Sluder, 2013). Instead, PCM proteins were suggested for centriole association during mitosis (Lee and Rhee, 2012; Matsuo et al., 2012; Pagan et al., 2015; Fry, 2015). We previously proposed that PCM integrity is essential for association of centrioles during mitosis (Seo et al., 2015). Since PCNT plays a critical role in PCM accumulation at the onset of mitosis (Fig. 1G–O) (Doxsey et al., 1994; Lee and Rhee, 2011; Kim and Rhee, 2014), we predicted that levels of PCNT expression may have a negative correlation with the rate of premature centriole separation. To examine our prediction, we generated *PCNT*-deleted cells rescued with ectopic expression of DD–FLAG–PCNT$^{S1235/1241A}$–Myc (PCNT^{AA}) in which PLK1 phosphorylation sites were substituted with alanine residues, resulting in no centrosome maturation (Lee and Rhee, 2011). Immunoblot analysis revealed that both wild-type and mutant ectopic PCNT proteins were expressed (Fig. 5A). However, immunostaining analysis revealed that the centrosomal levels of PCNT^{AA} were significantly lower than those of PCNT^{WT} in mitotic cells (Fig. 5B,C). Furthermore, the centrosomal levels of endogenous CEP215 were lower in PCNT^{AA}-rescued cells (Fig. 5B,D). In accordance with our prediction, the ectopic PCNT^{AA} mutant rescued centriole separation less efficiently than PCNT^{WT} (Fig. 5E,F). Most cells with associated centrioles had higher levels of centrosomal PCNT than those with separated centrioles (Fig. 5G,H). This phenomenon was observed in both the PCNT^{WT}- and PCNT^{AA}-rescued cells. In fact, we were able to estimate a threshold level of ectopic PCNT for centriole association and separation (Fig. 5H). These results imply that a critical amount of mitotic PCM is required for holding centrioles together during mitosis.

Prematurely separated centrioles did not convert to centrosomes

During mitotic exit, a daughter centriole acquires the ability to recruit PCM and to assemble a new centriole in the next cell cycle (Wang et al., 2011; Fu and Glover, 2016). This change was named centriole-to-centrosome conversion (Wang et al., 2011). It has been reported that selective centrosomal proteins, such as CEP135, CEP295, CEP192 and CEP152, are sequentially recruited to the daughter centriole in this process (Izquierdo et al., 2014; Fu et al., 2015; Chang et al., 2016). We immunostained these proteins in *PCNT*-deleted cells to determine whether prematurely separated and amplified centrioles convert to centrosomes at early M phase. CEP135, CEP295 and CEP192 were detected in all the centrioles in *PCNT*-deleted cells, although the CEP192 signals were significantly reduced (Fig. 6A–D). However, CEP152 signals were detected in only two centrioles among all the separated and amplified centrioles (Fig. 6A,E). Furthermore, all the CEP152 signals overlapped with CEP164, a marker for the mother centriole (Fig. 6F,G). However, the CEP152 signals showed a low degree of overlap with centrobin, a marker for the daughter centriole (Fig. 6H,I). We also observed that most of the centrioles were decorated with CEP152 signals only after mitosis, irrespective of the absence of PCNT (Fig. 6J,K). These results indicate that prematurely separated and amplified daughter centrioles are not yet converted to centrosomes at prometaphase.

Centrioles converted to centrosomes only after the removal of PCNT in G0/G1 cells

To determine the importance of PCNT cleavage for centriole-to-centrosome conversion during mitotic exit, we rescued the *PCNT*-deleted cells with ectopic expression of DD–FLAG–PCNT^{R2231A}–Myc (PCNT^{RA}), a mutant PCNT that is not cleaved by separase during mitotic exit (Lee and Rhee, 2012; Matsuo et al., 2012). Expression of ectopic PCNT was under the control of an inducible promoter that is activated by doxycycline. Immunoblot analysis revealed that comparable amounts of ectopic PCNT proteins were expressed (Fig. 7A). It is of note that no specific cleavage band was detected in the PCNT^{RA}-rescued cells (Fig. 7A). To observed the effect of PCNT cleavage on centriole separation during mitotic exit, we collected early G1 phase cells with the double thymidine block and release method (Fig. 7B). Immunostaining analysis detected lower levels of ectopic PCNT^{WT} than PCNT^{RA} at the centrosomes in cells exiting mitosis (Fig. 7C,D). The amount of endogenous CEP215 was also reduced in ectopic PCNT^{WT}-expressing cells in comparison to PCNT^{RA}-expressing cells (Fig. 7C,E). Furthermore, the PCNT^{WT}-expressing cells had separated centrioles, but those with PCNT^{RA} had associated centrioles (Fig. 7C,F). These results are consistent with previous reports that PCNT cleavage is necessary for centriole separation during mitotic exit (Lee and Rhee, 2012; Matsuo et al., 2012; Kim et al., 2015).

Next, we cultured the cells in serum-deprived medium so that most of them were arrested at G0/G1 phase. To remove ectopic PCNT from the cells, we washed out doxycycline and shield1 (Fig. 7G). Immunoblot analysis revealed that over 90% of ectopic proteins disappeared from the cells 6 h after the removal of

Journal of Cell Science (2019) 132, jcs225789. doi:10.1242/jcs.225789

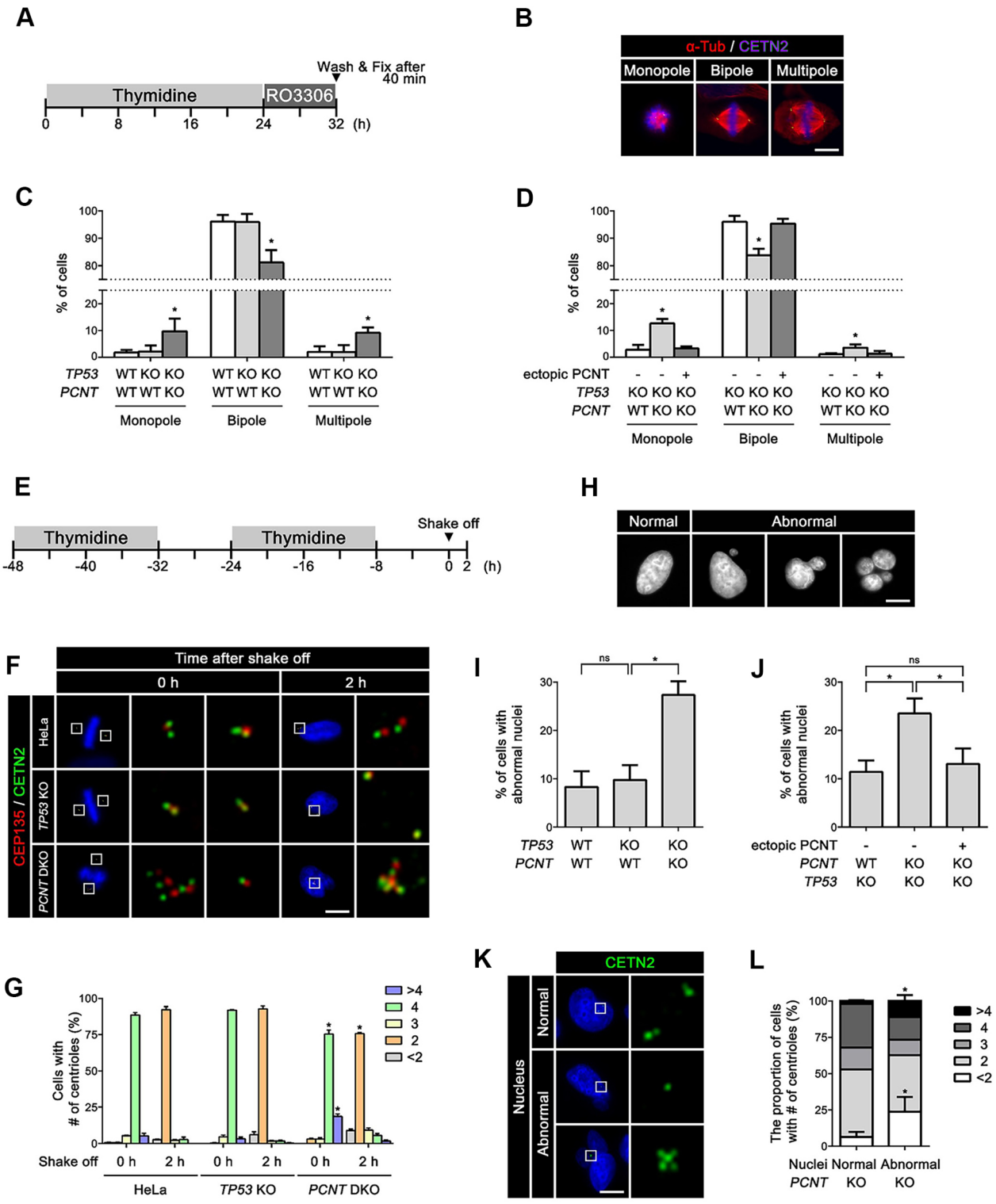

Fig. 2. Defects in spindle formation in *PCNT*-deleted cells. (A) Schematic illustrating how sequential treatment of thymidine-RO3306 and release allowed the cells to enter mitosis synchronously. (B) HeLa cells were co-immunostained with antibodies specific to α-tubulin (α-Tub, red) and centrin-2 (CETN2, green). (C,D) Abnormal spindle poles were counted in *PCNT* and *TP53* wild-type (WT) or knockout (KO) cells (C) and in cells rescued with expression of ectopic $PCNT^{WT}$ (DD–FLAG–PCNT–Myc) (D). (E) Schematic illustrating how mitotic cells were enriched with the double thymidine block and release. For G1 phase cells, mitotic cells were collected using a shake-off method and cultured for two additional hours. (F) Cells were co-immunostained with antibodies specific to centrin-2 (green) and CEP135 (red). Boxed area in left panels is magnified in the right panels. (G) The number of centrioles per cell as shown in F was counted. (H) Morphology of the interphase nuclei was determined with DAPI staining. (I,J) Abnormal nuclei as shown in H were counted in *PCNT*-deleted cells (I) and in cells rescued with expression of ectopic $PCNT^{WT}$ (J). (K) *PCNT*-deleted cells were immunostained with centrin-2 antibody (green). (L) The number of centrin-2 signals were counted in *PCNT*-deleted cells as shown in K with normal and abnormal nuclei. (B,F,H,K) DNA was visualized with DAPI (blue or gray). Scale bars: 10 µm. (C,D,G,I,J,L) >300 cells per group were analyzed in three independent experiments. Values are the means±s.d. One-way ANOVA (C,D,I,J) and unpaired two-tailed *t*-test (G,L) were used for statistical analyses. **P*<0.05; ns, not significant.

Journal of Cell Science (2019) 132, jcs225789. doi:10.1242/jcs.225789

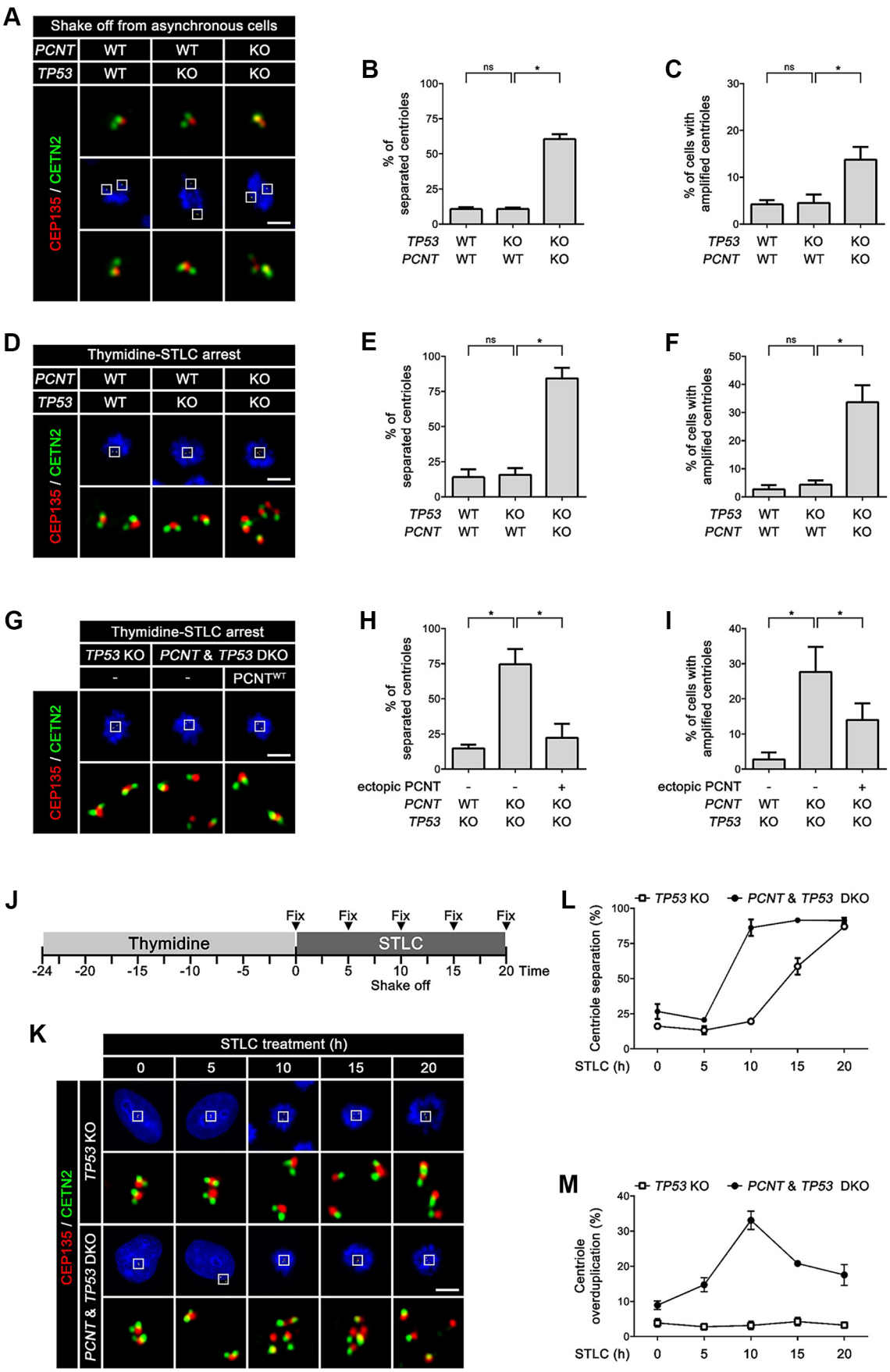

Fig. 3. See next page for legend.

Fig. 3. Premature centriole separation and amplification in *PCNT*-deleted mitotic cells. (A) Mitotic *PCNT* and *TP53* wild-type (WT) or knockout (KO) HeLa cells were collected from asynchronous populations using a shake-off method. Cells were co-immunostained with antibodies specific to centrin-2 (CETN2, green) and CEP135 (red). Boxed areas in middle panels are magnified in upper and lower panels. (B) Centriole separation was determined with a 1:1 ratio of the centrin-2 and CEP135 signals as shown in A. (C) Centriole amplification was determined with five or more centrin-2 signals per cell as shown in A. (D) Cells were arrested at prometaphase with sequential treatment of thymidine and STLC. Mitotic cells were co-immunostained with antibodies specific to centrin-2 (green) and CEP135 (red). Boxed area in upper panels is magnified in lower panels. (E,F) Centriole separation (E) and centriole amplification (F) were determined in cells as shown in D. (G) *PCNT*-deleted cells were rescued with expression of ectopic $PCNT^{WT}$ and co-immunostained with antibodies specific to centrin-2 (green) and CEP135 (red). (H,I) Centriole separation (H) and amplification (I) were determined in cells as shown in G. (J) Schematic illustrating how cells were arrested at S phase through treatment of thymidine and then released in the presence of STLC. The cells were collected every 5 h after the release from thymidine. Most cells entered mitosis 9 h after the STLC treatment. (K) Cells were co-immunostained with antibodies specific to centrin-2 (green) and CEP135 (red). (L,M) Centriole separation (L) and centriole overduplication (M) were determined in cells as shown in K. (A,D,G,K) DNA was visualized with DAPI (blue). Scale bars: 10 µm. (B,C,E,F,H,I,L,M) >300 cells per group were analyzed in three independent experiments. Values are the means±s.d. One-way ANOVA (B,C, E,F,H,I) was used for statistical analyses. **P*<0.05; ns, not significant.

doxycycline and shield1 (Fig. 7H). Under these conditions, approximately half of the cells expressing the cleavage-resistant $PCNT^{RA}$ mutant included separated centrioles within 8 h after washing out doxycycline and shield1, revealing that the removal of PCNT induced centriole separation in G0-arrested cells (Fig. 7I,J). We used super-resolution structured illumination microscopy (SR-SIM) to determine the centriolar localization of CEP152 in the G0-arrested cells. The results showed that only one out of two centrioles was surrounded by CEP152 in those rescued with $PCNT^{RA}$ (Fig. 7K,L). After degradation of $PCNT^{RA}$, both centrioles were surrounded by CEP152 (Fig. 7K,L). As a control, CEP152 signals were detected in both centrioles in the cells rescued with $PCNT^{WT}$ (Fig. 7K,L). These results suggest that the removal of PCNT is required not only for centriole separation but also for centriole-to-centrosome conversion during mitotic exit.

PCNT should be cleaved for centriole-to-centrosome conversion

To confirm a direct link between PCNT cleavage and centriole-to-centrosome conversion, we rescued the *PCNT*-deleted cells with ectopic expression of DD–FLAG–$PCNT^{RA\text{-}TEV}$–Myc ($PCNT^{RA\text{-}TEV}$), which is cleaved only by TEV protease (Fig. S7) (Kapust and Waugh, 2000). TEV protease in the SNIPer system becomes active only in the presence of rapamycin (Gray et al., 2010). In fact, $PCNT^{RA\text{-}TEV}$ was cleaved only in the presence of rapamycin when the cells were cultured in serum-deprived medium (Fig. 8A,B). Under these conditions, we observed that the number of cells with separated centrioles significantly increased with rapamycin treatment (Fig. 8C,D). We also observed centrosomal signals of CEP152 with SR-SIM. The results showed that activation of TEV protease induced an increase in the number of cells with both centrioles decorated with CEP152 (Fig. 8E,F). These results confirm that PCNT cleavage is necessary for centriole-to-centrosome conversion as well as for centriole separation during mitotic exit.

DISCUSSION

In this report, we analyzed centrosomal phenotypes of *PCNT*-deleted HeLa cells. It was surprising that the deletion of *PCNT* had little effect on interphase centrosomes. By contrast, *PCNT* deletion led to premature separation and amplification of centrioles in mitotic centrosomes. When a non-cleavable PCNT mutant ($PCNT^{RA}$) was gradually removed or artificially cleaved by TEV protease in G0-arrested knockout cells, centrioles started to separate from each other and convert to centrosomes. Our observations revealed the importance of PCNT in the regulation of centriole behavior during mitosis.

Daughter centrioles in interphase cells are orthogonally engaged with the mother centrioles, possibly through a glue protein whose identity remains unclear (Tsou et al., 2009; Schöckel et al., 2011; Oliveira and Nasmyth, 2013). Entering mitosis, a centriole pair disengages, and its members eventually separate from each other. Several lines of evidence indicate that centriole disengagement and separation occur in multiple steps. Loncarek and colleagues discovered that a daughter centriole creates a distance from the mother centriole right after mitotic entry (Shukla et al., 2015). We interpret that a centriole pair disengages at the moment when the daughter centriole departs from the wall of mother centriole. However, the disengaged centriole pair remains associated within the mitotic centrosome because it is surrounded by PCM proteins (Fig. 8G). It is known that separase-dependent cleavage of PCNT is a key event for centriole separation (Lee and Rhee, 2012; Matsuo et al., 2012). Specific cleavage of PCNT induces disintegration of PCM, and as a result, a centriole pair separates from each other. If PCNT was not cleaved, centrioles would remain associated within the centrosome even after mitosis (Fig. 8G). Therefore, we propose that some PCM proteins physically block the separation of a centriole pair (Fig. 8G). Consistent with this view, centrioles prematurely separate when mitotic PCM is dispersed by microtubule pulling forces (Cabral et al., 2013; Seo et al., 2015). Furthermore, loss of CEP215 causes premature centriole separation in mouse embryonic fibroblasts (Barrera et al., 2010). However, we do not rule out the possibility that PCNT itself may play a direct role in holding a centriole pair within the mitotic centrosome.

One of the most striking phenotypes in *PCNT*-deleted cells may be premature centriole separation and amplification in early mitosis. While preparing this manuscript, we learned that deletion of *PLP*, a *Drosophila* homolog of *PCNT*, also resulted in premature centriole separation and overduplication in sensory organ precursor cells (Roque et al., 2018). Premature centriole separation and amplification were observed in *PCNT*-depleted cells possibly because of the role of PCNT in centriole association (Lee and Rhee, 2011). It remains to be investigated what happens in cells with amplified centrioles. Cells with multiple centrioles might complete mitosis through an error-prone event called spindle pole clustering (Holland and Cleveland, 2009). As a result, a fraction of *PCNT*-deleted cells would retain multiple centrioles immediately after mitosis. The generation of nuclei with abnormal morphology may be one of the outcomes. We also observed that a fraction of the *PCNT*-deleted cells underwent apoptosis, probably as a result of multiple centrioles in interphase cells.

A mother centriole is known to have the potential to assemble a new centriole once it disengages from an existing daughter centriole (Loncarek et al., 2008; Shukla et al., 2015). However, we and others did not observe a significant increase in centriole amplification in disengaged but associated centrioles during mitosis. Centrioles were amplified only when a daughter centriole was liberated from the mother centriole. It is possible that mitotic PCM may prevent a mother centriole from being exposed to centriole assembly cues, such as PLK1 and PLK4 (Loncarek et al., 2008; Shukla et al., 2015; Novak et al., 2016). Once a mother centriole is free of the

Journal of Cell Science (2019) 132, jcs225789. doi:10.1242/jcs.225789

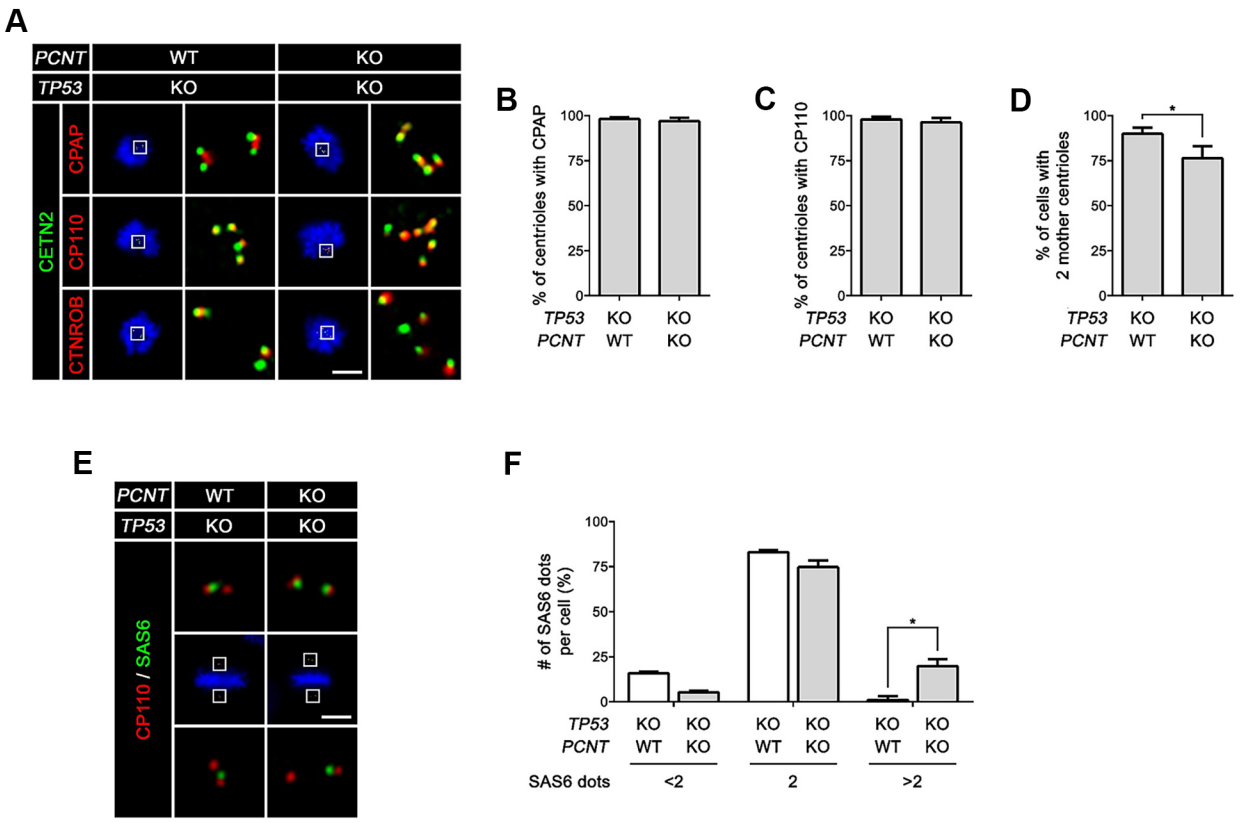

Fig. 4. Amplification of daughter centrioles in *PCNT*-deleted cells during mitosis. (A) *PCNT* and *TP53* wild-type (WT) or knockout (KO) HeLa cells were arrested at prometaphase with sequential treatment of thymidine and STLC. Mitotic cells were co-immunostained with antibodies specific to centrin-2 (CETN2, green), CPAP (red), CP110 (red), and centrobin (CNTROB, red). Boxed area in left panels is magnified in the right panels. (B,C) Proportion of the centrin-2-positive centrioles as shown in A that co-immunostained with CPAP (B) and CP110 (C) were determined. (D) The number of cells as shown in A with only a pair of centrobin-negative (mother) centrioles was counted. (E) Cells were enriched at M phase with double thymidine block and release and co-immunostained with antibodies specific to CP110 (red) and SAS6 (green). Boxed areas in middle panels are magnified in upper and lower panels. (F) The number of SAS6 signals per cell was counted in cells as shown in E. (A,E) DNA was visualized with DAPI (blue). Scale bar: 10 µm. (B–D,F) >300 centrosomes per group were analyzed in three independent experiments. Values are the means±s.d. Unpaired two-tailed *t*-test was used for statistical analyses. **P*<0.05.

surrounding PCM, it may have better access to centriole assembly cues. It was recently reported that the CDK1–cyclin B complex binds STIL and prevents phosphorylation by PLK4 during mitosis (Zitouni et al., 2016). It remains to be investigated why a fraction of centrioles in *PCNT*-deleted mitotic cells amplify during the CDK1–cyclin B-rich mitotic phase. It is possible that the CDK1–cyclin B complex has a better access to the centriole pair, which is surrounded by mitotic PCM. As the mitotic PCM disengages from centrioles in *PCNT*-deleted cells, a fraction of them may be exposed to PLK4 and initiate centriole assembly. Centrioles in mitotically arrested cells may not be exposed to PLK4 to the same degree as they are surrounded by mitotic PCM.

When a daughter centriole separates from a mother centriole during mitotic exit, it becomes a young mother centriole, acquiring the ability to assemble a new centriole in the next round of the cell cycle (Wang et al., 2011). It is interesting that a daughter centriole becomes a mother centriole only after mitotic exit. In the absence of PCNT, the amplified centrioles in prometaphase-arrested cells may be intact, as we detected all the tested centriole markers, including SAS6. However, they are not converted into the centrosome at this stage, as exemplified by a lack of CEP152 (Fig. 6). Based on these results, we propose that centriole separation is necessary but not sufficient for centriole-to-centrosome conversion. Rather, a centriole must experience mitotic exit for conversion to a centrosome. It is possible that a novel factor is required for the induction of centriole-to-centrosome conversion, which may be activated only after cells exit mitosis. Therefore, future studies should focus on identifying this factor for centriole-to-centrosome conversion.

MATERIALS AND METHODS

Cell culture and cell cycle synchronization

The Flp-In T-REx HeLa cells (generously gifted by Dr Stephen Taylor, University of Manchester, UK) were cultured in DMEM (Welgene, LM 001-05) supplemented with 10% FBS (Welgene, S101-01) and antibiotics (Invivogen, ANT-MPT) at 37°C and 5% CO_2. All cell lines were regularly tested for mycoplasma contamination test with mycoplasma PCR detection kit (CellSafe, CS-D-50).

To synchronize cell cycles, we used 2 mM thymidine (Sigma-Aldrich, T9250), 5 µM STLC (Tocris, 2191), 50 ng/ml nocodazole (Sigma-Aldrich, M1404), 5 µM paclitaxel (Sigma-Aldrich, T7402) and 5 µM RO-3306 (Enzo Life Sciences, ALX-270-463-M005).

Generation of *PCNT* and *TP53* double knockout cell lines

Knockout cell lines were generated using CRISPR/Cas9 technique as described previously (Sander and Joung, 2014). The *TP53* genes were deleted prior to the *PCNT* genes. The guide RNA sequences of *PCNT* (5′-GAC GGC ATT GAC GGA GCT GC GGG-3′) and *TP53* (5′-CCG GTT CAT GCC GCC CAT GC AGG-3′) were used. In brief, 2.4×10^5 cells were seeded on a 60 mm dish and transfected with *pSpCAS9(BB)-2A-Puro* vector (Addgene, 48139) containing a guide RNA sequence of the target gene. One day after transfection, cells were optionally transferred to a 100 mm dish and

Journal of Cell Science (2019) 132, jcs225789. doi:10.1242/jcs.225789

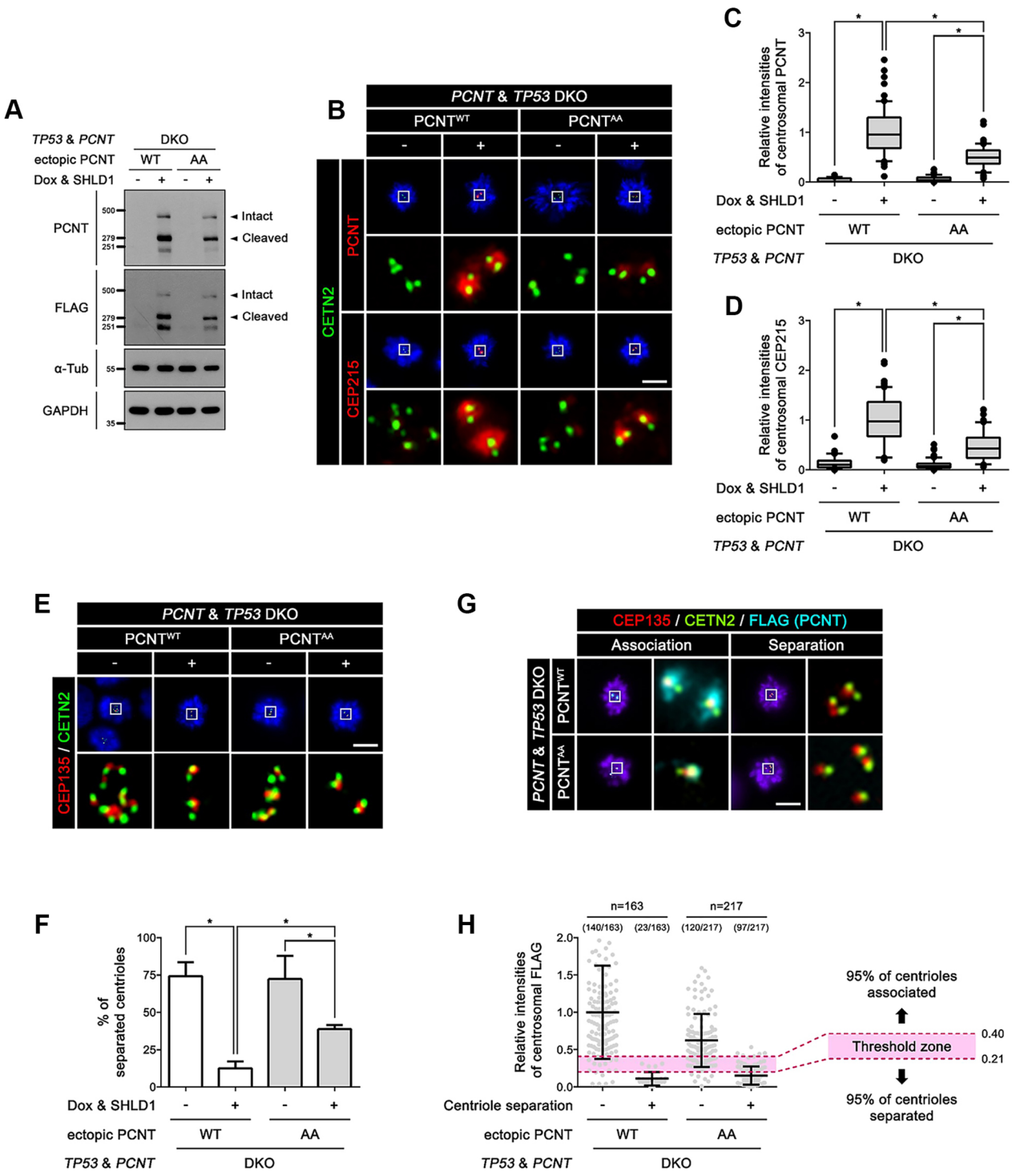

Fig. 5. Importance of mitotic PCM for centriole association. (A) Expression of ectopic PCNT^{WT} (DD–FLAG–PCNT–Myc) and PCNT^{AA} (DD–FLAG–PCNT$^{S1235/1241A}$–Myc) in *PCNT* and *TP53* double knockout (DKO) HeLa cells was confirmed by means of immunoblot analyses for PCNT, FLAG, α-tubulin (α-Tub) and GAPDH. (B) STLC-arrested cells were co-immunostained with antibodies specific to centrin-2 (green), PCNT (red) and CEP215 (red). Doxycycline and shield1 treatment (+) was used or not (–) to induce expression of the ectopic PCNT proteins. Boxed area in upper panels is magnified in lower panels. (C,D) Intensities of the centrosomal PCNT (C) and CEP215 (D) signals as shown in B are represented with box and whisker plots. >60 centrosomes per group were analyzed in three independent experiments. (E) *PCNT*-deleted cells were rescued with PCNT^{WT} or PCNT^{AA} and subjected to co-immunostaining analysis with antibodies specific to CEP135 (red) and centrin-2 (green). (F) Centriole separation was determined in cells as shown in E. >300 centrosomes per group were analyzed in three independent experiments. Values are the means±s.d. (G) Rescued cells were co-immunostained with antibodies specific to CEP135 (red), centrin-2 (green) and FLAG (cyan). Boxed area in left panels is magnified in the right panels. (H) Centrosomal intensities of the ectopic PCNT (FLAG) in cells as shown in G were measured in associated and separated centrioles. >150 centrosomes per group were analyzed in three independent experiments. Values are the means±s.d. The threshold zone divides the centrosomal FLAG intensities with strong correlations with centriole association (above threshold zone) and separation (below threshold zone). Gray circles indicate each measured value. (B,E,G) DNA was visualized with DAPI (blue or violet). Scale bars: 10 µm. (C,D,F) Two-way ANOVA was performed for statistical analysis. *P<0.05.

Journal of Cell Science

Journal of Cell Science (2019) 132, jcs225789. doi:10.1242/jcs.225789

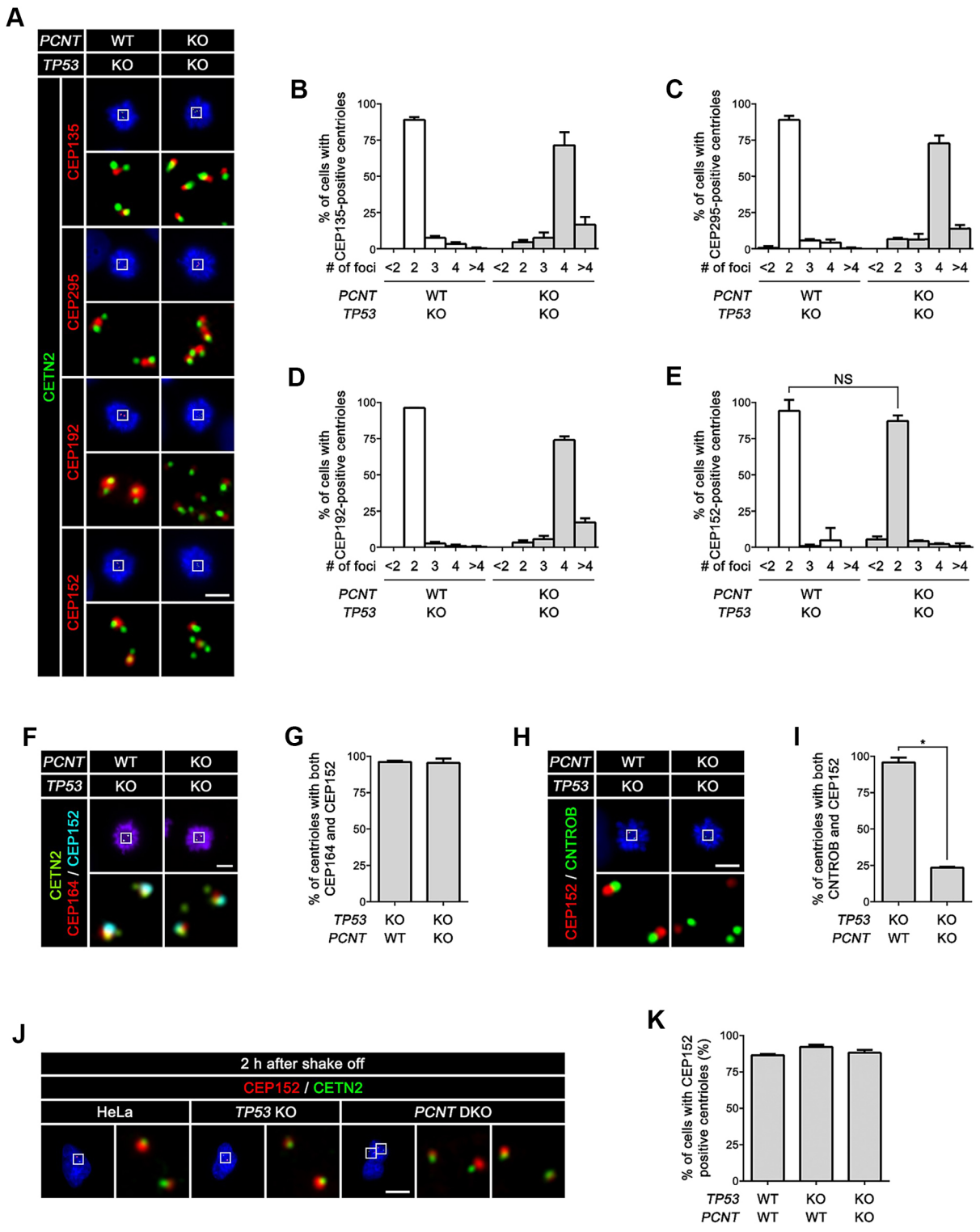

Fig. 6. Prematurely separated and amplified daughter centrioles are devoid of CEP152. (A) STLC-arrested *PCNT* and *TP53* wild-type (WT) or knockout (KO) HeLa cells were subjected to co-immunostaining analysis with antibodies specific to centrin-2 (CETN2, green) along with CEP135, CEP295, CEP192 or CEP152 (red). Boxed area in upper panels is magnified in lower panels. (B–E) The number of centriolar signals of CEP135 (B), CEP295 (C), CEP192 (D) and CEP152 (E) per cell as shown in A was counted. (F) Cells were co-immunostained with antibodies specific to centrin-2 (green), CEP164 (red) and CEP152 (cyan). (G) The number of centrioles with both CEP164 and CEP152 signals per cells as shown in F was counted. (H) Cells were co-immunostained with antibodies specific to CEP152 (red) and centrobin (CNTROB, green). (I) The number of centrioles with both centrobin and CEP152 signals in cells as shown in H was counted. (J) Cells in G1 phase were co-immunostained with antibodies specific to CEP152 (red) and centrin-2 (green). Boxed area in left panels is magnified in the right panels. (K) The number of centrioles with CEP152 signals in cells as shown in J was counted. (A,F,H,J) DNA was visualized with DAPI (blue or violet). Scale bar: 10 µm. (B–E,G,I,K) >300 cells per group were analyzed in three independent experiments. Values are the means±s.d. Unpaired two-tailed *t*-test was used for statistical analyses. **P*<0.05; NS, not significant.

Journal of Cell Science (2019) 132, jcs225789. doi:10.1242/jcs.225789

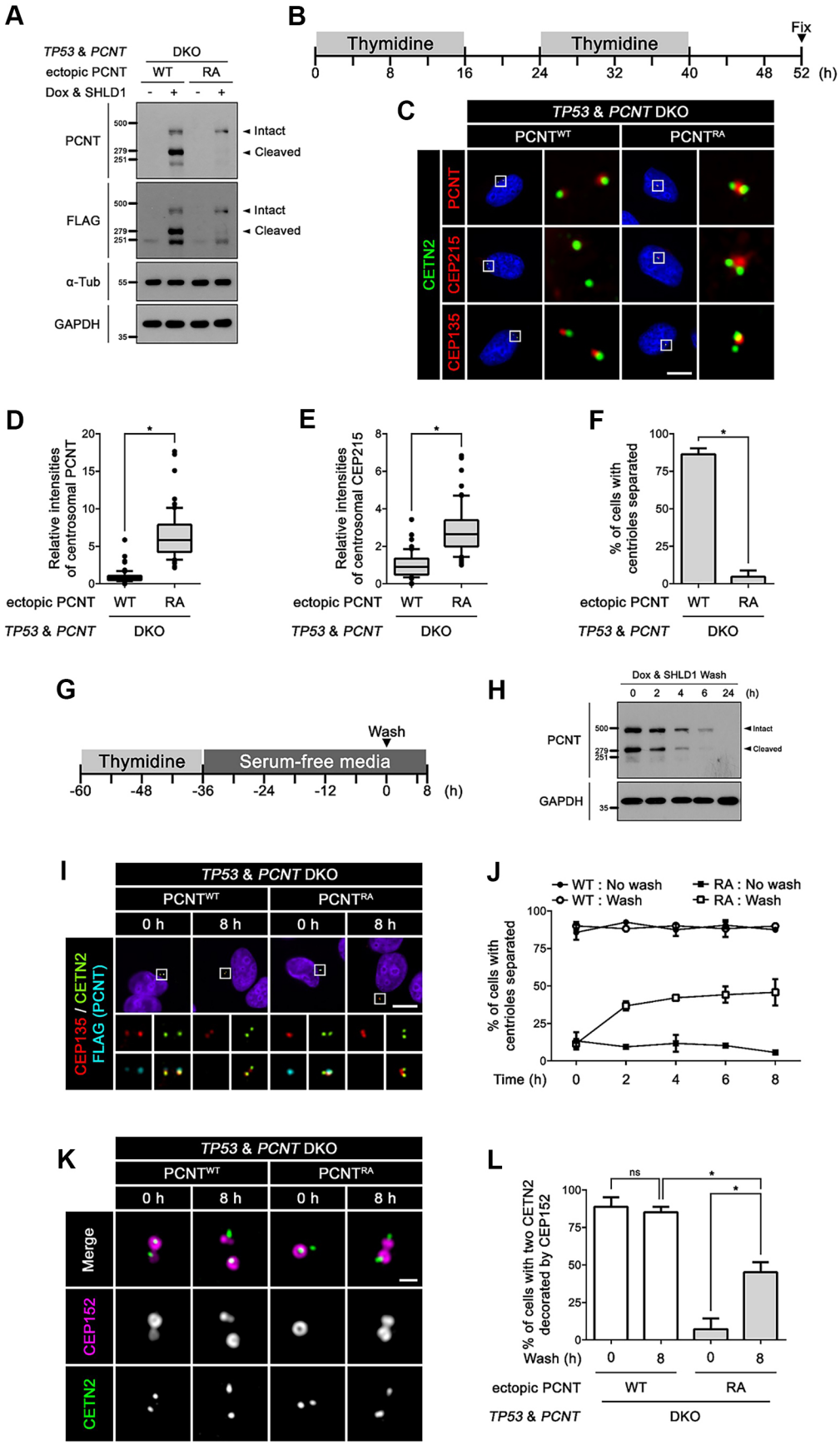

Fig. 7. Centriole separation after removal of PCNT. (A) Expression of ectopic PCNT^{WT} and PCNT^{RA} in *PCNT* and *TP53* double knockout (DKO) HeLa cells was confirmed by means of immunoblot analyses. Doxycycline and shield1 treatment was used to induce expression of the ectopic PCNT proteins. (B) Schematic illustrating how cells were enriched at early G1 phase with a double thymidine block and release. (C) Immunocytochemistry was performed with antibodies specific to centrin-2 (green), PCNT (red), CEP215 (red), and CEP135 (red). Boxed area in left panels is magnified in the right panels. (D,E) Intensities of the centrosomal PCNT (D) and CEP215 (E) signals as shown in C are represented with box and whisker plots. >60 centrosomes per group were analyzed in three independent experiments. (F) Centriole separation was determined in cells as shown in C. >300 cells per group were analyzed in three independent experiments. (G) Schematic illustrating how PCNT^{WT}- and PCNT^{RA}-rescued cells were cultured in serum-deprived medium for enrichment at G0 phase. Expression of the ectopic PCNT proteins was suppressed through the removal of doxycycline and shield1. (H) Immunoblot analysis was performed to determine cellular levels of PCNT^{WT} after the removal of doxycycline and shield1. (I) Eight hours after removal, immunocytochemistry was performed with antibodies specific to CEP135 (red), centrin-2 (green) and FLAG (cyan). Boxed area in upper panels is magnified in lower panels. (J) Centriole separation was determined in the PCNT^{WT}- and PCNT^{RA}-rescued cells as shown in I after the removal of doxycycline and shield1. >300 cells per group were analyzed in three independent experiments. (K) Cells were co-immunostained with antibodies specific to centrin-2 (green) and CEP152 (magenta) and observed with SR-SIM microscopy. Scale bar: 0.5 µm. (L) Cells as shown in K with a pair of CEP152-positive centrioles were counted. >100 cells per group were analyzed in three independent experiments. (C,I) DNA was visualized with DAPI (blue or violet). Scale bars: 10 µm. (F,J,L) Values are the means±s.d. (D–F,L) Unpaired two-tailed *t*-test (D–F) and two-way ANOVA (L) were used for statistical analyses. **P*<0.05; ns, not significant.

Journal of Cell Science (2019) 132, jcs225789. doi:10.1242/jcs.225789

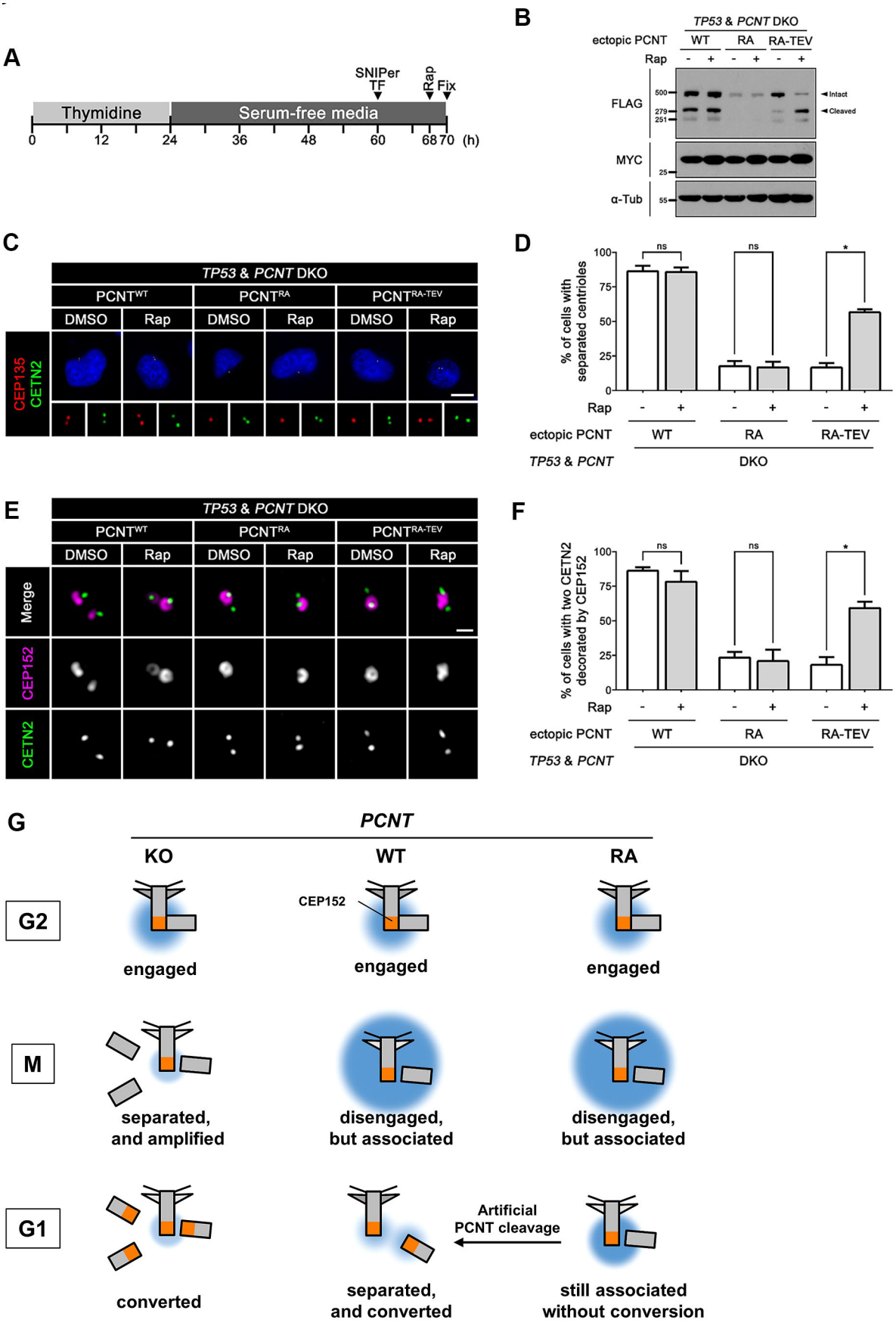

Fig. 8. See next page for legend.

Fig. 8. Centriole-to-centrosome conversion after induction of PCNT cleavage. (A) Schematic illustrating how *PCNT*-deleted cells were rescued with expression of ectopic $PCNT^{WT}$, $PCNT^{RA}$ or $PCNT^{RA\text{-}TEV}$ (DD–FLAG–$PCNT^{R2231A\text{-}TEV}$–Myc) and cultured in a serum-deprived medium for enrichment at G0 phase. The *SNIPer* plasmids were introduced for activation of TEV protease with rapamycin (Rap). (B) Immunoblot analysis was performed to determine specific cleavage of $PCNT^{RA\text{-}TEV}$ in *PCNT* and *TP53* double knockout (DKO) HeLa. TEV protease was detected by means of anti-Myc antibody. (C) Cells were co-immunostained with antibodies specific to centrin-2 (green) and CEP135 (red). Scale bar: 10 µm. (D) Centriole separation was determined in G0 phase cells as shown in C. >300 cells per group were analyzed in three independent experiments. (E) Centriolar localization of CEP152 (magenta) was analyzed with SR-SIM. Scale bar: 0.5 µm. (F) The number of cells as shown in E with a pair of CEP152-positive centrioles was counted. >100 cells per group were analyzed in three independent experiments. (D,F) Values are the means±s.d. Two-way ANOVA was used for statistical analyses. **P*<0.05; ns, not significant. (G) Model for roles of PCM in mitotic centrosomes. Entering mitosis, the mother and daughter centrioles are disengaged from each other but remain associated within PCM. At the end of mitosis, a daughter centriole separates from the mother centriole and becomes a young mother centriole. In the absence of PCNT, a pair of centrioles prematurely separates and frequently amplifies at prometaphase. However, daughter centrioles do not become young mother centrioles yet. In the case of $PCNT^{RA}$, a centriole pair remains associated even after mitosis. Artificial cleavage of $PCNT^{RA}$ allows centriole separation and centriole-to-centrosome conversion in G0 phase.

treated with 0.5 mg/ml puromycin (Calbiochem, 540222) for 3–5 days. Monoclonal cell lines were established with the dilution cloning method and indel types of target genes were analyzed.

Establishment of inducible PCNT expression and degradation system

To regulate PCNT expression and degradation, we simultaneously applied *pcDNA™5/FRT/TO* and ProteoTuner systems. The destabilization domain of pTRE-Cycle1 vector (Clontech Laboratories, 631115) was attached to all FLAG–PCNT–Myc constructs, and the new construct subcloned into *pcDNA™5/FRT/TO* vector (Invitrogen, V6520-20). To induce Flp recombinase-mediated integration, *pOG44* (Invitrogen, V6005-20) and *pcDNA™5/FRT/TO* vectors containing a PCNT construct were cotransfected into Flp-In T-REx HeLa cells in which both the *PCNT* and *TP53* genes were deleted. DNA transfection was performed with FugeneHD (Promega, E2311) according to manufacturer's protocol. After transfection, cells were treated with 0.1 mg/ml hygromycin B (Calbiochem, 400051) for 2–3 weeks and then monoclonal cell lines were established with the dilution cloning method. To induce and stabilize ectopic PCNT proteins, cells were treated with 10 ng/ml doxycycline (Sigma-Aldrich, D9891) and 50 nM shield1 (Clontech Laboratories, 632189). To reduce leaky expression of ectopic proteins, Tet system approved FBS (Clontech Laboratories, 631107) was used.

SNIPer system for artificial PCNT cleavage

To regulate PCNT cleavage in TEV-dependent manner, we generated cell lines expressing DD–FLAG–$PCNT^{R2231A\text{-}TEV}$–Myc ($PCNT^{RA\text{-}TEV}$) in which the TEV consensus sequence of ENLYFQS was inserted into DD–FLAG–$PCNT^{R2231A}$–Myc next to the mutated R2231A residue. We cotransfected SNIPer plasmids (FRB-N-TEV in *pQCXIP* and FKBP-C-TEV 219 in *pQCXIH*) using Lipofectamine 3000 reagent (Invitrogen, L3000008) according to manufacturer's protocol. 8 h after transfection, 10 nM rapamycin (Sigma-Aldrich, R8781) was added for 2 h to activate TEV protease.

Antibodies

The antibodies specific to CEP135 [immunocytochemistry (ICC) 1:2000; Kim et al., 2008], CEP215 [ICC 1:2000, immunoblot (IB) 1:500; Lee and Rhee, 2010], PCNT (ICC 1:2000, IB 1:2000; Kim and Rhee, 2011), CP110 (ICC 1:100; Chang et al., 2010), CPAP (ICC 1:100; Chang et al., 2010) and centrobin (ICC 1:200; Jeong et al., 2007) were previously described. Antibodies specific to centrin-2 (Merck Millipore, 04-1624; ICC 1:1000), CEP295 (Abcam, 122490; ICC 1:500), CEP192 (Bethyl Laboratories, A302-324A; ICC 1:1000, IB 1:500), CEP152 (Abcam, 183911; ICC 1:500), GAPDH (Life Technologies, AM4300; IB 1:20,000), α-tubulin (Abcam, ab18251; ICC 1:2000, IB 1:20,000), γ-tubulin (Abcam, 11316; ICC 1:1000, IB 1:2000) were purchased. Secondary antibodies conjugated with fluorescent dye (Alexa Fluor 488, 594 and 647; Life Technologies, ICC 1:1000) and with horseradish peroxidase (Sigma-Aldrich or Millipore, IB 1:10,000) were purchased.

Immunoblot analyses

The cells were lysed on ice for 10 min with RIPA buffer (150 mM NaCl, 1% Triton X-100, 0.5% sodium deoxycolate, 0.1% SDS, 50 mM Tris-HCl at pH 8.0, 10 mM NaF, 1 mM Na_3VO_4, 1 mM EDTA and 1 mM EGTA) containing a protease inhibitor cocktail (Sigma-Aldrich, P8340) and centrifuged with 13,400 ***g*** for 10 min at 4°C. The supernatants were mixed with 4× SDS sample buffer (250 mM Tris-HCl at pH 6.8, 8% SDS, 40% glycerol and 0.04% Bromophenol Blue) and 10 mM DTT (Amresco, 0281-25G). Mixtures were boiled for 5 min. To detect intact and cleaved PCNT, 15–20 mg of proteins were loaded in SDS polyacrylamide gel (3% stacking gel and 4.5% separating gel), electrophoresed and transferred to Protran BA85 nitrocellulose membranes (GE Healthcare Life Sciences, 10401196). The membranes were blocked with blocking solution (5% nonfat milk in 0.1% Tween 20 in TBS or 5% bovine serum albumin in 0.1% Tween 20 in TBS) for 2 h, incubated with primary antibodies diluted in blocking solution for 16 h at 4°C, washed four times with TBST (0.1% Tween 20 in TBS), incubated with secondary antibodies in blocking solution for 30 min and washed again. To detect the signals of secondary antibodies, ECL reagent (ABfrontier, LF-QC0101) and X-ray films (Agfa, CP-BU NEW) were used. In the cases of other proteins, 5% stacking and 10–18% separating gels were used. Uncropped film images of immunoblot are provided in Fig. S8.

Immunostaining analysis

For immunocytochemistry, cells seeded on cover glass (Marienfeld, 0117520) were fixed with cold methanol for 10 min and washed three times with cold PBS. In the case of mitotic cells, cover slips were coated with poly-L-lysine (Sigma-Aldrich, P4707) for 10 min and all reagents were not directly poured onto it during fixation. After incubation of PBST (0.1% Triton X-100 in PBS) for 10 min, the cells were blocked with blocking solution (3% bovine serum albumin, and 0.3% Triton X-100 in PBS) for 30 min, incubated with primary antibodies diluted in blocking solution for 1 h, washed three times with PBST, incubated with secondary antibodies in blocking solution for 30 min, washed twice with PBST, incubated with 4,6-diamidino-2-phenylindole (DAPI) solution for 3 min and washed twice with PBST. The cover glasses were mounted on a slide glass with ProLong Gold antifade reagent (Life Technologies, P36930). Images were acquired from fluorescence microscopes equipped with digital cameras (Olympus IX51 equipped with QImaging QICAM Fast 1394 or Olympus IX81 equipped with ANDOR iXonEM+) and processed in ImagePro 5.0 (Media Cybernetics) or MetaMorph 7.6 (Molecular Devices). We scanned all focal planes to count centrin-2 signals per cell. Inset images were enlarged four times in ImageJ 1.51k (National Institutes of Health) using the bicubic interpolation option. In cases of quadruple staining, the Image 5D plugin of ImageJ was used for pseudo-coloring.

To obtain super-resolution images, we used structured illumination microscopy (Carl Zeiss ELYRA PS.1 equipped with Plan-Apochromat 63×/1.40 Oil DIC objective and ANDOR iXon 885 EMCCD camera). The images were taken with serial *z*-stack sectioning with 250 nm intervals. SIM processing was performed in ZEN software 2012, black edition (Carl Zeiss).

To measure fluorescence intensities, we immunostained all cells at the same time with the same diluent antibodies. All images were captured at same exposure time without stopping. ImageJ 1.51k was used to measure fluorescence intensities at centrosomes. In each measurement, background signals were subtracted from the sum of fluorescence signals at centrosomes.

Statistical analysis

For statistical analyses, experiments were independently performed three times. To calculate *P*-values, unpaired two-tailed *t*-test, one- or two-way

analysis of variance (ANOVA) were performed in Prism 6 (GraphPad Software). In the case of ANOVA, the Tukey's post-test was performed if *P*-value was lower than 0.05.

All measured fluorescence intensities were displayed with box-and-whiskers plots in Prism 6 (lines, median; vertical boxes, values from 25th and 75th; down error bars, 10th value, up error bar, 90th value; circle, outliers).

Acknowledgements
We thank Dr Jim Wells (University of California, San Francisco, USA) for generously providing us with the *SNIPer* plasmids. This research was supported by the Basic Science Research Program through the National Research Foundation of Korea funded by the Ministry (NRF-2014R1A4A1005259 and 2016R1A2B4009418).

Competing interests
The authors declare no competing or financial interests.

Author contributions
Conceptualization: Jaeyoun Kim, K.R.; Methodology: Jaeyoun Kim, Jeongjin Kim, K.R.; Software: Jaeyoun Kim, Jeongjin Kim; Validation: Jaeyoun Kim; Formal analysis: K.R.; Investigation: Jaeyoun Kim, Jeongjin Kim, K.R.; Data curation: K.R.; Writing - original draft: Jaeyoun Kim, K.R.; Writing - review & editing: Jaeyoun Kim, K.R.; Visualization: Jaeyoun Kim, Jeongjin Kim, K.R.; Supervision: K.R.; Project administration: K.R.; Funding acquisition: K.R.

Funding
This research was supported by the Basic Science Research Program through the National Research Foundation of Korea funded by the Ministry (NRF-2014R1A4A1005259 and 2016R1A2B4009418).

Supplementary information
Supplementary information available online at
http://jcs.biologists.org/lookup/doi/10.1242/jcs.225789.supplemental

References
Arquint, C. and Nigg, E. A. (2016). The PLK4-STIL-SAS-6 module at the core of centriole duplication. *Biochem. Soc. Trans.* **44**, 1253-1263.
Arquint, C., Gabryjonczyk, A.-M., Imseng, S., Böhm, R., Sauer, E., Hiller, S., Nigg, E. A. and Maier, T. (2015). STIL binding to Polo-box 3 of PLK4 regulates centriole duplication. *eLife* **4**, e07888.
Banaszynski, L. A., Chen, L.-C., Maynard-Smith, L. A., Ooi, A. G. L. and Wandless, T. J. (2006). A rapid, reversible, and tunable method to regulate protein function in living cells using synthetic small molecules. *Cell* **126**, 995-1004.
Barrera, J. A., Kao, L. R., Hammer, R. E., Seemann, J., Fuchs, J. L. and Megraw, T. L. (2010). CDK5RAP2 regulates centriole engagement and cohesion in mice. *Dev. Cell* **18**, 913-926.
Bettencourt-Dias, M., Rodrigues-Martins, A., Carpenter, L., Riparbelli, M., Lehmann, L., Gatt, M. K., Carmo, N., Balloux, F., Callaini, G. and Glover, D. M. (2005). SAK/PLK4 is required for centriole duplication and flagella development. *Curr. Biol.* **15**, 2199-2207.
Cabral, G., Sans, S. S., Cowan, C. R. and Dammermann, A. (2013). Multiple mechanisms contribute to centriole separation in C. elegans. *Curr. Biol.* **23**, 1380-1387.
Chang, J., Cizmecioglu, O., Hoffmann, I. and Rhee, K. (2010). PLK2 phosphorylation is critical for CPAP function in procentriole formation during the centrosome cycle. *EMBO J.* **29**, 2395-2406.
Chang, C.-W., Hsu, W.-B., Tsai, J.-J., Tang, C.-J. C. and Tang, T. K. (2016). CEP295 interacts with microtubules and is required for centriole elongation. *J. Cell Sci.* **129**, 2501-2513.
Cizmecioglu, O., Arnold, M., Bahtz, R., Settele, F., Ehret, L., Haselmann-Weiss, U., Antony, C. and Hoffmann, I. (2010). Cep152 acts as a scaffold for recruitment of Plk4 and CPAP to the centrosome. *J. Cell Biol.* **191**, 731-739.
Conduit, P. T., Wainman, A. and Raff, J. W. (2015). Centrosome function and assembly in animal cells. *Nat. Rev. Mol. Cell Biol.* **16**, 611-624.
Delaval, B. and Doxsey, S. (2008). Genetics: dwarfism, where pericentrin gains stature. *Science* **319**, 732-733.
Doxsey, S. J., Stein, P., Evans, L., Calarco, P. D. and Kirschner, M. (1994). Pericentrin, a highly conserved centrosome protein involved in microtubule organization. *Cell* **76**, 639-650.
Dzhindzhev, N. S., Yu, Q. D., Weiskopf, K., Tzolovsky, G., Cunha-Ferreira, I., Riparbelli, M., Rodrigues-Martins, A., Bettencourt-Dias, M., Callaini, G. and Glover, D. M. (2010). Asterless is a scaffold for the onset of centriole assembly. *Nature* **467**, 714-718.
Dzhindzhev, N. S., Tzolovsky, G., Lipinszki, Z., Schneider, S., Lattao, R., Fu, J., Debski, J., Dadlez, M. and Glover, D. M. (2014). Plk4 phosphorylates Ana2 to trigger Sas6 recruitment and procentriole formation. *Curr. Biol.* **24**, 2526-2532.
Egeler, E. L., Urner, L. M., Rakhit, R., Liu, C. W. and Wandless, T. J. (2011). Ligand-switchable substrates for a ubiquitin-proteasome system. *J. Biol. Chem.* **286**, 31328-31336.
Fong, C. S., Mazo, G., Das, T., Goodman, J., Kim, M., O'Rourke, B. P., Izquierdo, D. and Tsou, M.-F. B. (2016). 53BP1 and USP28 mediate p53-dependent cell cycle arrest in response to centrosome loss and prolonged mitosis. *eLife* **5**, e16270.
Fry, A. M. (2015). Solving the centriole disengagement puzzle. *Nat. Cell Biol.* **17**, 3-5.
Fu, J. and Glover, D. (2016). How the newborn centriole becomes a mother. *Cell Cycle* **15**, 1521-1522.
Fu, J., Lipinszki, Z., Rangone, H., Min, M., Mykura, C., Chao-Chu, J., Schneider, S., Dzhindzhev, N. S., Gottardo, M., Riparbelli, M. G. et al. (2015). Conserved molecular interactions in centriole-to-centrosome conversion. *Nat. Cell Biol.* **18**, 87-99.
Gray, D. C., Mahrus, S. and Wells, J. A. (2010). Activation of specific apoptotic caspases with an engineered small-molecule-activated protease. *Cell* **142**, 637-646.
Habedanck, R., Stierhof, Y.-D., Wilkinson, C. J. and Nigg, E. A. (2005). The Polo kinase Plk4 functions in centriole duplication. *Nat. Cell Biol.* **7**, 1140-1146.
Hatch, E. M., Kulukian, A., Holland, A. J., Cleveland, D. W. and Stearns, T. (2010). Cep152 interacts with Plk4 and is required for centriole duplication. *J. Cell Biol.* **191**, 721-729.
Holland, A. J. and Cleveland, D. W. (2009). Boveri revisited: chromosomal instability, aneuploidy and tumorigenesis. *Nat. Rev. Mol. Cell Biol.* **10**, 478-487.
Holland, A. J., Lan, W., Niessen, S., Hoover, H. and Cleveland, D. W. (2010). Polo-like kinase 4 kinase activity limits centrosome overduplication by autoregulating its own stability. *J. Cell Biol.* **188**, 191-198.
Izquierdo, D., Wang, W. J., Uryu, K. and Tsou, M. F. (2014). Stabilization of cartwheel-less centrioles for duplication requires CEP295-mediated centriole-to-centrosome conversion. *Cell Rep.* **8**, 957-965.
Jeong, Y., Lee, J., Kim, K., Yoo, J. C. and Rhee, K. (2007). Characterization of NIP2/centrobin, a novel substrate of Nek2, and its potential role in microtubule stabilization. *J. Cell Sci.* **120**, 2106-2116.
Kapust, R. B. and Waugh, D. S. (2000). Controlled intracellular processing of fusion proteins by TEV protease. *Protein Expr. Purif.* **19**, 312-318.
Karki, M., Keyhaninejad, N. and Shuster, C. B. (2017). Precocious centriole disengagement and centrosome fragmentation induced by mitotic delay. *Nat. Commun.* **8**, 15803.
Kim, K. and Rhee, K. (2011). The pericentriolar satellite protein CEP90 is crucial for integrity of the mitotic spindle pole. *J. Cell Sci.* **124**, 338-347.
Kim, S. and Rhee, K. (2014). Importance of the CEP215-pericentrin interaction for centrosome maturation during mitosis. *PLoS ONE* **9**, e87016.
Kim, K., Lee, S., Chang, J. and Rhee, K. (2008). A novel function of CEP135 as a platform protein of C-NAP1 for its centriolar localization. *Exp. Cell Res.* **314**, 3692-3700.
Kim, T.-S., Park, J.-E., Shukla, A., Choi, S., Murugan, R. N., Lee, J. H., Ahn, M., Rhee, K., Bang, J. K., Kim, B. Y. et al. (2013). Hierarchical recruitment of Plk4 and regulation of centriole biogenesis by two centrosomal scaffolds, Cep192 and Cep152. *Proc. Natl. Acad. Sci. USA* **110**, E4849-E4857.
Kim, J., Lee, K. and Rhee, K. (2015). PLK1 regulation of PCNT cleavage ensures fidelity of centriole separation during mitotic exit. *Nat. Commun.* **6**, 10076.
Kitagawa, D., Busso, C., Flückiger, I. and Gönczy, P. (2009). Phosphorylation of SAS-6 by ZYG-1 is critical for centriole formation in C. elegans embryos. *Dev. Cell* **17**, 900-907.
Kitagawa, D., Vakonakis, I., Olieric, N., Hilbert, M., Keller, D., Olieric, V., Bortfeld, M., Erat, M. C., Flückiger, I., Gönczy, P. et al. (2011). Structural basis of the 9-fold symmetry of centrioles. *Cell* **144**, 364-375.
Kratz, A.-S., Barenz, F., Richter, K. T. and Hoffmann, I. (2015). Plk4-dependent phosphorylation of STIL is required for centriole duplication. *Biol. Open* **4**, 370-377.
Lambrus, B. G., Daggubati, V., Uetake, Y., Scott, P. M., Clutario, K. M., Sluder, G. and Holland, A. J. (2016). A USP28-53BP1-p53-p21 signaling axis arrests growth after centrosome loss or prolonged mitosis. *J. Cell Biol.* **214**, 143-153.
Lawo, S., Hasegan, M., Gupta, G. D. and Pelletier, L. (2012). Subdiffraction imaging of centrosomes reveals higher-order organizational features of pericentriolar material. *Nat. Cell Biol.* **14**, 1148-1158.
Lee, S. and Rhee, K. (2010). CEP215 is involved in the dynein-dependent accumulation of pericentriolar matrix proteins for spindle pole formation. *Cell Cycle* **9**, 775-784.
Lee, K. and Rhee, K. (2011). PLK1 phosphorylation of pericentrin initiates centrosome maturation at the onset of mitosis. *J. Cell Biol.* **195**, 1093-1101.
Lee, K. and Rhee, K. (2012). Separase-dependent cleavage of pericentrin B is necessary and sufficient for centriole disengagement during mitosis. *Cell Cycle* **11**, 2476-2485.
Lee, M., Seo, M. Y., Chang, J., Hwang, D. S. and Rhee, K. (2017). PLK4 phosphorylation of CP110 is required for efficient centriole assembly. *Cell Cycle* **16**, 1225-1234.
Loncarek, J. and Bettencourt-Dias, M. (2017). Building the right centriole for each cell type. *J. Cell Biol.* **217**, 823-835.

Loncarek, J., Hergert, P., Magidson, V. and Khodjakov, A. (2008). Control of daughter centriole formation by the pericentriolar material. *Nat. Cell Biol.* **10**, 322-328.
Matsuo, K., Ohsumi, K., Iwabuchi, M., Kawamata, T., Ono, Y. and Takahashi, M. (2012). Kendrin is a novel substrate for separase involved in the licensing of centriole duplication. *Curr. Biol.* **22**, 915-921.
Meitinger, F., Anzola, J. V., Kaulich, M., Richardson, A., Stender, J. D., Benner, C., Glass, C. K., Dowdy, S. F., Desai, A., Shiau, A. K. et al. (2016). 53BP1 and USP28 mediate p53 activation and G1 arrest after centrosome loss or extended mitotic duration. *J. Cell Biol.* **214**, 155-166.
Mennella, V., Keszthelyi, B., McDonald, K. L., Chhun, B., Kan, F., Rogers, G. C., Huang, B. and Agard, D. A. (2012). Subdiffraction-resolution fluorescence microscopy reveals a domain of the centrosome critical for pericentriolar material organization. *Nat. Cell Biol.* **14**, 1159-1168.
Moyer, T. C., Clutario, K. M., Lambrus, B. G., Daggubati, V. and Holland, A. J. (2015). Binding of STIL to Plk4 activates kinase activity to promote centriole assembly. *J. Cell Biol.* **209**, 863-878.
Nigg, E. A. and Holland, A. J. (2018). Once and only once: mechanisms of centriole duplication and their deregulation in disease. *Nat. Rev. Mol. Cell Biol.* **19**, 297-312.
Novak, Z. A., Wainman, A., Gartenmann, L. and Raff, J. W. (2016). Cdk1 phosphorylates Drosophila Sas-4 to recruit polo to daughter centrioles and convert them to centrosomes. *Dev. Cell* **37**, 545-557.
O'Connell, K. F., Caron, C., Kopish, K. R., Hurd, D. D., Kemphues, K. J., Li, Y. and White, J. G. (2001). The C. elegans zyg-1 gene encodes a regulator of centrosome duplication with distinct maternal and paternal roles in the embryo. *Cell* **105**, 547-558.
Ohta, M., Ashikawa, T., Nozaki, Y., Kozuka-Hata, H., Goto, H., Inagaki, M., Oyama, M. and Kitagawa, D. (2014). Direct interaction of Plk4 with STIL ensures formation of a single procentriole per parental centriole. *Nat. Commun.* **5**, 5267.
Oliveira, R. A. and Nasmyth, K. (2013). Cohesin cleavage is insufficient for centriole disengagement in Drosophila. *Curr. Biol.* **23**, R601-R603.
Pagan, J. K., Marzio, A., Jones, M. J. K., Saraf, A., Jallepalli, P. V., Florens, L., Washburn, M. P. and Pagano, M. (2015). Degradation of Cep68 and PCNT cleavage mediate Cep215 removal from the PCM to allow centriole separation, disengagement and licensing. *Nat. Cell Biol.* **17**, 31-43.
Rauch, A., Thiel, C. T., Schindler, D., Wick, U., Crow, Y. J., Ekici, A. B., van Essen, A. J., Goecke, T. O., Al-Gazali, L., Chrzanowska, K. H. et al. (2008). Mutations in the pericentrin (PCNT) gene cause primordial dwarfism. *Science* **319**, 816-819.
Roque, H., Saurya, S., Pratt, M. B., Johnson, E. and Raff, J. W. (2018). Drosophila PLP assembles pericentriolar clouds that promote centriole stability, cohesion and MT nucleation. *PLoS Genet.* **14**, e1007198.
Sander, J. D. and Joung, J. K. (2014). CRISPR-Cas systems for editing, regulating and targeting genomes. *Nat. Biotechnol.* **32**, 347-355.
Schöckel, L., Möckel, M., Mayer, B., Boos, D. and Stemmann, O. (2011). Cleavage of cohesin rings coordinates the separation of centrioles and chromatids. *Nat. Cell Biol.* **13**, 966-972.
Seo, M. Y., Jang, W. and Rhee, K. (2015). Integrity of the pericentriolar material is essential for maintaining centriole association during M phase. *PLoS ONE* **10**, e0138905.
Shukla, A., Kong, D., Sharma, M., Magidson, V. and Loncarek, J. (2015). Plk1 relieves centriole block to reduplication by promoting daughter centriole maturation. *Nat. Commun.* **6**, 8077.
Sluder, G. (2013). Centriole engagement: it's not just cohesin any more. *Curr. Biol.* **23**, R659-R660.
Sonnen, K. F., Schermelleh, L., Leonhardt, H. and Nigg, E. A. (2012). 3D-structured illumination microscopy provides novel insight into architecture of human centrosomes. *Biol. Open* **1**, 965-976.
Strnad, P., Leidel, S., Vinogradova, T., Euteneuer, U., Khodjakov, A. and Gönczy, P. (2007). Regulated HsSAS-6 levels ensure formation of a single procentriole per centriole during the centrosome duplication cycle. *Dev. Cell* **13**, 203-213.
Tsou, M.-F. B. and Stearns, T. (2006). Mechanism limiting centrosome duplication to once per cell cycle. *Nature* **442**, 947-951.
Tsou, M.-F. B., Wang, W.-J., George, K. A., Uryu, K., Stearns, T. and Jallepalli, P. V. (2009). Polo kinase and separase regulate the mitotic licensing of centriole duplication in human cells. *Dev. Cell* **17**, 344-354.
Tsuchiya, Y., Yoshiba, S., Gupta, A., Watanabe, K. and Kitagawa, D. (2016). Cep295 is a conserved scaffold protein required for generation of a bona fide mother centriole. *Nat. Commun.* **7**, 12567.
van Breugel, M., Hirono, M., Andreeva, A., Yanagisawa, H.-A., Yamaguchi, S., Nakazawa, Y., Morgner, N., Petrovich, M., Ebong, I.-O., Robinson, C. V. et al. (2011). Structures of SAS-6 suggest its organization in centrioles. *Science* **331**, 1196-1199.
Wang, W.-J., Soni, R. K., Uryu, K. and Tsou, M.-F. (2011). The conversion of centrioles to centrosomes: essential coupling of duplication with segregation. *J. Cell Biol.* **193**, 727-739.
Woodruff, J. B., Wueseke, O. and Hyman, A. A. (2014). Pericentriolar material structure and dynamics. *Philos. Trans. R. Soc. Lond. B Biol. Sci.* **369**, 20130459.
Zitouni, S., Francia, M. E., Leal, F., Montenegro Gouveia, S., Nabais, C., Duarte, P., Gilberto, S., Brito, D., Moyer, T., Kandels-Lewis, S. et al. (2016). CDK1 Prevents Unscheduled PLK4-STIL Complex Assembly in Centriole Biogenesis. *Curr. Biol.* **26**, 1127-1137.